Appl. Phys. B 71, 795–800 (2000) / Digital Object Identifier (DOI) 10.1007/s003400000419

Applied Physics B
Lasers
and Optics

Femtosecond pump-probe investigation of ultrafast silver nanoparticle deformation in a glass matrix

G. Seifert, M. Kaempfe, K.-J. Berg, H. Graener

Fachbereich Physik, Martin-Luther-Universität Halle-Wittenberg, 06099 Halle, Germany
(Fax: +49-345/552-7221, E-mail: g.seifert@physik.uni-halle.de)

Received: 3 April 2000/Revised version: 3 July 2000/Published online: 20 September 2000 –

Abstract. Single-color femtosecond pump-probe experiments were performed to investigate the time dependence of laser-induced ultrafast desorption and deformation processes of silver nanoparticles in glass. After laser excitation at wavelengths close to the surface plasmon resonance, transient extinction changes were found to exhibit dynamics on quite different time scales ranging from sub-picoseconds to some hundred ps. The slowest observed decay component is identified as characteristic for the deformation/desorption processes. Possible mechanisms for these processes are discussed.

PACS: 78.40Pg; 78.47+w

In the last years a variety of studies using ultrashort laser pulses were performed on the properties of metal and semiconductor nanoclusters. Depending on the surroundings of the nanoparticles, ultrafast processes have been investigated, for example electron relaxation and the consecutive energy thermalization in rigid matrices [1–5], two-photon photoionization [6] or laser-induced fragmentation of free clusters in vacuum and liquid matrix [7]. Applying high intensities, also permanent optical modifications were reported [8, 9]. In particular, recently permanent color changes leading to dichroism were observed in samples of glass containing silver nanoparticles upon irradiation with intense fs laser pulses, where the optical axis of the produced dichroism was found to depend on the polarization direction of the laser [10, 11]. By help of transmission electron microscopy it could be shown that these effects are due to deformation and partial fragmentation of the silver particles within the glass matrix [11, 12]. In this letter we report first fs pump-probe experiments which were performed in order to find the characteristic time scales and possible mechanisms of these ultrafast desorption and deformation processes.

1 Experimental

The experiments were carried out on samples of commercial flat glass of usual chemical composition [13] containing spherical silver nanoparticles with a rather broad range of sizes in a surface region of approximately 30 μm thickness. These samples were prepared by Na^+/Ag^+ ion exchange below the glass transformation temperature T_g and subsequent annealing in hydrogen gas (also at $T < T_g$). The radii of the particles produced by this procedure range from typically 5 nm close to the glass surface up to ≈ 50 nm in a depth of 30 μm. The volume concentration of the particles also varies significantly with the depth below the glass surface up to a maximum value of $\approx 10^{-3}$. These particles' surface plasmon (SP) resonances lead to a strong and rather broad absorption band, which is seen as the prominent feature in the solid curve of Fig. 1, which represents the initial spectrum of the samples used in this work. The maximum extinction of the SP resonance band is located at $\lambda = 411$ nm, its full width at half maximum being approximately 45 nm; the extinction below $\lambda = 340$ nm is due to the glass matrix.

Single-frequency fs pump-probe experiments were performed on these samples using the second harmonic of a titanium:sapphire laser (pulse duration ≈ 150 fs; pulse shape sech^2 in good approximation). The results discussed below were obtained using linearly polarized pulses having wavelengths between 390 nm and 420 nm; in this wavelength range preferably the smallest particles close to the surface are affected, as could be proven studying the intensity dependence of permanent optical changes [11]. The pump en-

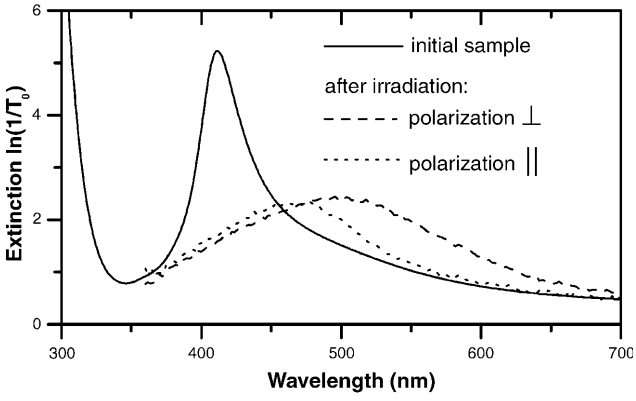

Fig. 1. Extinction spectrum of the initial sample (*solid line*), and typical spectra from the center of an irradiated spot, measured with polarization parallel (*dotted curve*) and perpendicular (*dashed curve*) to the laser polarization

ergy densities at the sample were varied between 0.025 and 2.5 J/cm^2, while the probe fluence was below 0.01 J/cm^2 in every case. In the current setup the maximum delay between pump and probe pulse was 1 ns. The polarization directions of pump and probe pulses were chosen perpendicular to each other to avoid scattering background; the results should be comparable to the case of measuring with parallel polarization directions, because at wavelengths around 400 nm the permanent transmission changes are not polarization dependent [10]. This can also be seen looking at the dashed and dotted curves in Fig. 1, which give typical sample spectra after irradiation by a single femtosecond pulse (at $\lambda = 400$ nm) measured in the center of an irradiated spot with light polarized parallel (dotted) and perpendicular (dashed) to the laser polarization [10]. The beam diameter of the probe pulses was adjusted to approximately half that of the pump pulses. The reason for this choice is that the investigated processes are known to have a significant and particularly nonlinear intensity dependence, with the consequence that the spatial average of transmission changes registered by the probe beam must be expected to be an average over different dynamics, too. To reduce this influence without allowing the probe pulses to permanently modify the sample themselves, the narrowed probe beam was the best compromise. As any sample area exposed to a single focused pump pulse is irreversibly modified, the sample has to be moved to a new position after each laser shot. Addressing this complication, the following experimental procedure was applied to achieve satisfactory data quality: First, with the pump beam being blocked, the initial energy transmission T_0 of a "fresh" sample area is measured. Then a single pump pulse is irradiated onto the sample, and the transient transmission $T(t_{\mathrm{Del}})$ is registered for the current delay time t_{Del} between pump and probe pulse. As third step the new stationary transmission T_{stat} of the modified sample area is measured typically 1 s after the laser-induced modification. At this time even the slowest dynamics within the sample, i.e. thermal diffusion (on a ms time scale) is finished. Finally the sample is moved and the whole cycle is repeated. Each data point obtained by this procedure yields both the transient and the stationary (long time) extinction changes of the sample, defined by $\ln(T(t_{\mathrm{Del}})/T_0)$ and $\ln(T_{\mathrm{stat}}/T_0)$. It should be noted that, due to this definition, bleaching (extinction decrease) is characterized by positive values. For the data presented below, the transmission changes were averaged over 15 laser shots at each delay position resulting in an absolute experimental accuracy of the order of 0.02 for an individual data point.

2 Results

In the following some characteristic time-resolved results measured by the above described method will be presented. As a first example Fig. 2 shows on four different time scales (from Fig. 2a to 2d the shown delay range is enlarged by roughly a factor of 10 in each step) the transient extinction changes as a function of delay time measured at $\lambda = 400$ nm for two different excitation energies: the full points refer to a total energy density per pulse of approximately 2.5 J/cm^2, the open squares to 0.5 J/cm^2. In Fig. 2a a pump-probe correlation for the applied 150-fs pulses (calculated assuming sech^2-shape, arbitrary amplitude) is given as solid line for

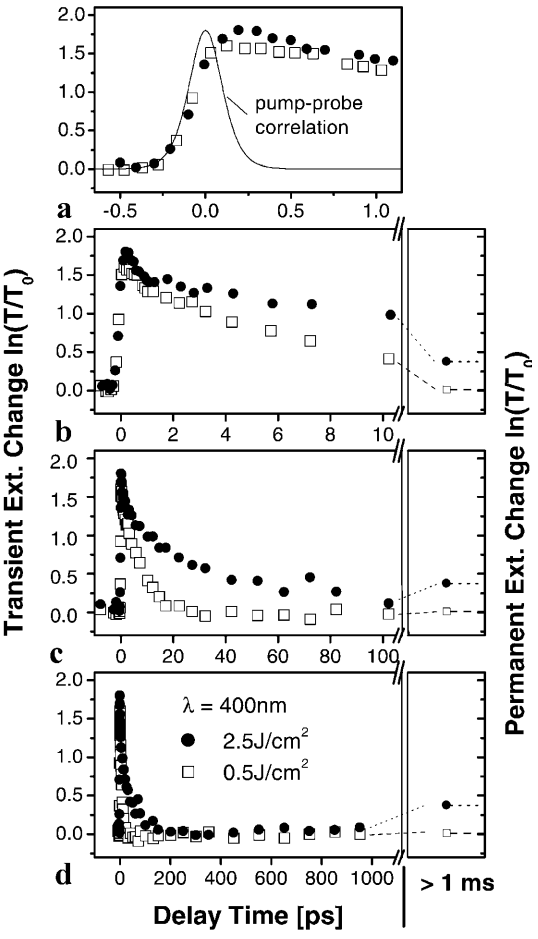

Fig. 2a–d. Transient extinction changes at $\lambda_{\mathrm{pump}} = \lambda_{\mathrm{probe}} = 400$ nm; excitation energy density per pulse ≈ 2.5 J/cm^2 (*solid circles*) and ≈ 0.5 J/cm^2 (*open squares*), respectively; *solid curve* in **a**: pump-probe correlation; **a** to **d** give the same data, only the scale of time axis is increased in each step by roughly a factor of 10; after the axis break in **b** to **d** the observed value of the permanent extinction change is plotted using the same symbols

comparison. Additionally in Figs. 2b–2d the average values of the measured stationary extinction changes are given in the right-hand part of each figure after the break of the time axes. It is easily seen that the higher energy density (solid circles) causes a considerable permanent bleaching (extinction decrease) of 0.37 ± 0.01, whereas reduction of the excitation energy by a factor of 5 already decreases this steady-state extinction change to a very low average value of 0.012 ± 0.005.

Discussing now the transient behavior from top to bottom, i.e. from shorter to longer time scales, the first important observation that can be made for both data sets in Fig. 2a is

Table 1. Decay constants and maximum value of $\ln(T/T_0)$ obtained at $\lambda = 400$ nm as function of relative intensity (maximum corresponds to 2.5 J/cm^2)

Relative intensity	Time constant/ps	max. $\ln(T/T_0)$
1.00	30.0 ± 2.5	1.80
0.43	9.6 ± 0.5	1.65
0.20	8.0 ± 0.4	1.60
0.09	7.1 ± 0.3	1.45

the rather flat increase of $\ln(T/T_0)$ leading to a maximum at a delay time of approximately 200 fs. The other striking finding is the very similar amplitude of the two curves despite their significantly different excitation energy. This indicates a significant level of saturation being present, in accordance with the fact that already more than half of the initial extinction $\ln(1/T_0) \approx 3$ at 400 nm is bleached in the maximum of the time-resolved data. Taking additional data into account (measured with pump energy densities of ≈ 0.22 and 1.1 J/cm^2, not shown here), it can be stated that a decrease of excitation energy by a factor of 11 results in a decrease of maximum bleaching by only 20%. The corresponding numbers are given in the right-hand column of Table 1. On the longer time scales, more prominent differences can be seen. Looking at Fig. 2b, two components can be recognized in the decay of the individual signals after their maximum bleaching: first a quite fast decay (which is more distinct for the higher pump intensity) is observed up to a delay time of ≈ 1.5 ps, then the decrease of $\ln(T/T_0)$ is becoming considerably slower, particularly in case of the higher pump energy. The decay of $\ln(T/T_0)$ of all four mentioned data sets was analyzed fitting the curves by a sum of two exponentials in the delay time interval from 0.5 to 20 ps. The fast component can only be distinctly recognized for the two highest energy densities, where a common time constant of ≈ 500 fs is obtained. The slower component yields decay constants increasing from ≈ 7 ps to ≈ 30 ps with increasing pump energy; these values and their estimated accuracy are collected in Table 1. The further time evolution, as given in Figs. 2c and 2d, depends strongly on the applied excitation energy: at the lower value of 0.5 J/cm^2 (open squares) within experimental accuracy the extinction change reaches its stationary value already at a delay time of approximately 30 ps. At the higher pump energy (solid circles) the extinction change drops below its long time value after roughly 50 ps, even reaches zero after ≈ 300 ps and finally begins to rise again on a rather slow time scale of several hundred ps. Obviously this increase is by no means finished at 1 ns, because the extinction change is still clearly below its stationary value, which must of course be reached in the end.

In Fig. 3, the high-energy result of Fig. 2, which was obtained at 400 nm (plotted as open circles in Fig. 3) is compared with data measured at similar energy densities, but different wavelengths: solid squares refer to pump and probe wavelength of 420 nm, full triangles to 390 nm. Again the stationary extinction changes are given as dotted lines marked by the appropriate symbol on the right-hand side; note the two breaks of the time axis denoting (i) the change from linear to logarithmic scale at 12 ps, and (ii) the end of the really measured delay time (the right part of the figure again only presents the measured steady-state values). All three curves show a bleaching peak around zero delay; the different amplitudes show the same trend as the initial extinction coefficients at the individual spectral position within the SP band; a similar statement also holds for the stationary changes. The further time evolution of the upper and lower curve in Fig. 3 differs significantly from that of the middle one (which was already discussed above): at 420 nm (squares), after a first fast decay the signal slightly increases again, and then decreases more slowly down to its long-time value, but does not fall below its final value (at least within the measured delay range). In contrast to this, at 390 nm the extinction change drops below its stationary value after 10 ps, and even takes negative values after 40 ps. These data directly allow the quite general conclusion that the observed "slow" dynamics (time scale of some 100 ps) can not be explained by variation of the SP band amplitude only. Instead at least a significant modification of its spectral shape must be present transiently; but also the occurrence of additional bands must be considered.

In order to find out more about the initial process of bleaching, which seems not to follow the pulse correlation, but to integrate over the excitation pulse, the time evolution of the rise of the bleaching was investigated as a function of pump energy at $\lambda = 400$ nm. Figure 4 gives four characteristic examples covering an energy density range of a factor of 20. It should be noted that even at the highest value of approximately 0.5 J/cm^2 hardly any permanent bleaching was observed. The slightly smaller maximum bleaching in this

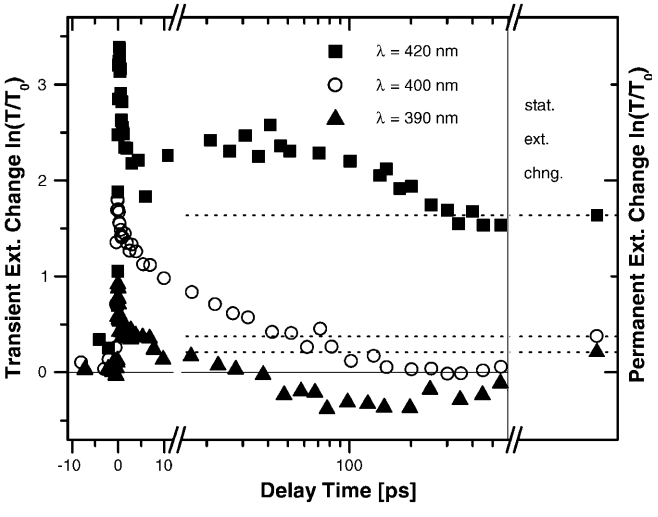

Fig. 3. Transient extinction changes at $\lambda_{pump} = \lambda_{probe} = 420$ nm (*solid squares*), 400 nm (*open circles*), and 390 nm (*triangles*); *dashed horizontal lines*: steady-state values of extinction change, marked by the appropriate symbols on the right margin; note the two axis breaks: the first marks the time scale change from linear to logarithmic, the second separates the steady-state regime

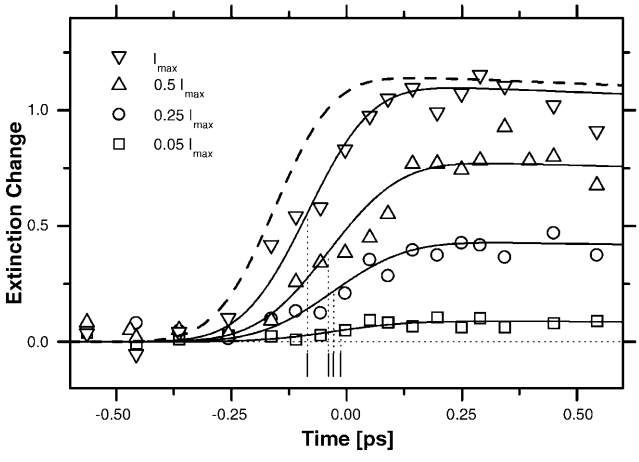

Fig. 4. Time evolution of extinction change at 400 nm for four different excitation intensities; the maximum intensity I_{max} corresponds to an energy density of ≈ 0.5 J/cm^2; experimental points, calculated curves; see text for details

series as compared to the data of Fig. 2 indicates a slightly different experimental situation, most probably due to different focal diameters. The following features can be stated for the extinction changes plotted in Fig. 4: (i) in all cases $\ln(T/T_0)$ increases within typically 500 fs from zero to its maximum value $A_{\max}$, and (ii) $A_{\max}$ increases monotonically, but obviously not linearly with intensity. If the signal rise is analyzed in more detail, for example, by fitting a usual step function to the increase of the data from zero to the maximum bleaching, in particular the point of half height (i.e. the delay time, where $A_{\max}/2$ is reached) and the steepness of the increase can be extracted. As indicated by the vertical lines in Fig. 4, the half-height position shifts to earlier times by nearly 100 fs upon increase from lowest to highest pump energy. The (normalized) steepness of the step remains unchanged within experimental accuracy. The solid and dashed curves in Fig. 4 are not the result of a fit of a really adequate theory to the data, but refer to the numerical solution of a simple three-level rate equation scheme; these curves will be explained and discussed below.

3 Interpretation

For an interpretation of the presented data it is helpful to recapitulate the state of knowledge about the ultrafast dynamics of metallic nanoparticles dispersed in condensed matter. In this field a variety of time-resolved experiments have been performed, but up to now only such results were reported, where no permanent modifications of the sample occurred. However, no matter if the irradiation of ultrashort laser pulses leads to permanent modifications of the sample or not, the initial interaction is the excitation of surface plasmons of the considered metal particles. These plasmons are known to dephase within less than 10 fs [14, 15]; in the next step the electronic system thermalizes due to electron–electron interaction [16]. This leads to an increase of the electron temperature on a 100-fs time scale resulting in a broadening of the SP absorption band [4]. The excess energy of the hot electron system is then transferred to the silver lattice via electron–phonon coupling on a time scale of several ps resulting in a hot particle. The time constant of this decay process was observed to increase with increasing intensity [16, 17]. Additionally in some cases volume oscillations of the nanoparticle having oscillation periods in the order of 10 ps have been reported [18–21]. As last step of the equilibration usually the transfer of the excess energy from the particle into the matrix is discussed, which typically requires 10 to 100 ps [16].

In principle, all these steps must also be present, when irreversible modifications of the extinction band are made (as in the experiments described above). These permanent optical changes have been found to be caused by partial fragmentation and, depending on particle size and distribution, deformation to non-spherical shapes [10–12]. So it is an obvious conclusion that observed differences between time-resolved experiments with and without permanent modifications should be characteristic for the processes of particle reshaping (this notion will in the following be used for both deformation and fragmentation). For the present data there is an easy way to distinguish between these two cases: the observation of a stationary bleaching can be taken as an indicator for permanent changes of the particle shapes, because the modification of the initially spherical particles leads to a redshift of the absorption band and thus to a steady-state extinction decrease at any wavelength used in this work [10, 11]. If, for example, the data of Fig. 2 are considered, the curve obtained at the lower energy density ($0.5\,\mathrm{J/cm^2}$) shows a very small, but still resolvable permanent bleaching. So this energy density may be regarded as the "upper limit" of the reversible regime, whereas the data measured at higher energy clearly represent the irreversible case. As the most prominent differences between these two curves are found at delay times of > 30 ps, the occurrence of the "slow" dynamics, i.e. particularly the observed variation of the extinction on a several hundred ps time scale in the case of the higher pump energy can be attributed to particle reshaping. Additional information about these slow processes can be concluded from the quite different behavior at different wavelengths as observed for the data of Fig. 3. Obviously there is a dynamic shift and/or broadening of the extinction band on this time scale, which might be due to energy transfer into and heating of the glass matrix. But also new absorption bands may arise dynamically if, for example, the silver particles are ionized.

In the delay range of 2 to 30 ps no unambiguous distinction between reversible and irreversible processes is possible: in principle the observed trend to slower decay with increasing pump energy is in agreement with the trend reported for electron–phonon coupling without particle modification in the literature [16, 17]. However, it can not be decided from the present data if the ≈ 30 ps decay constant found in this delay range for the presented $2.5\,\mathrm{J/cm^2}$ data set is just the continuation of this trend, or can, at least partially, be attributed to beginning particle modification.

It was already mentioned that the sub-ps decay component observable in Fig. 2 at delay times between the maximum bleaching and ≈ 2 ps is only visible at energy densities above $1.0\,\mathrm{J/cm^2}$; possibly this indicates a fast process (for example ejection of electrons) which is characteristic for the experimental situation that leads to particle reshaping.

Dynamical information on the time scale of 100 fs or faster can not be obtained directly from the presented data. However, processes on this time scale are obviously connected with the observed delayed rise of bleaching around zero delay. This delayed increase of transmission with respect to the pulse correlation function (compare Fig. 2a) was already observed at very low energy densities of $100\,\mu\mathrm{J/cm^2}$ and explained by SP resonance shift and broadening as a consequence of alteration of the dielectric function [22]. The important additional findings from the data presented here, namely shift of the rise to earlier times with increasing intensity (Fig. 3) and small variation of the bleaching amplitude at high intensities (see Table 1) are rather typical for saturation phenomena. In particular, the maximum values of $\ln(T/T_0)$ observed in Figs. 2 and 4 indicate that the initial extinction at 400 nm is bleached by more than 50% at delay times around 250 fs. Considering the integration over the beam profiles, the maximum extinction change should even be larger, i.e. the experimental situation is not far away from total bleaching. To check the plausibility of this idea, the situation was described by a strongly simplified model using a three-level rate equation system. In this description, the initial situation is taken as ground state. The upper state represents excited surface plasmons of the silver particles, which are considered as ideal harmonic oscillator, i.e. the extinction band is assumed to re-

main unchanged upon SP excitation. In the model, transient spectral changes (due to modification of the SP band) are treated as relaxation with a decay constant τ_{fast} into a third, intermediate level, where the system is assumed to provide no absorption at the laser wavelength. Physically, this level describes the situation of a thermalized electron system, but with nearly no energy being transferred to silver lattice and glass matrix. The latter processes are characterized by a relaxation step back down to the ground state with a time constant τ_{slow}. To be able to describe saturation for a certain duration t_{p} of the excitation pulse, it is necessary to choose $\tau_{\text{fast}} < t_{\text{p}}$ and $\tau_{\text{slow}} \gg t_{\text{p}}$. In particular, we chose $\tau_{\text{fast}} = t_{\text{p}}/20$, since the process leading to extinction changes is not explicitly specified in the model, and it should not be excluded that also transient spectral changes on a 10-fs time scale could be involved. For the slow process $\tau_{\text{slow}} = 100t_{\text{p}}$ was used to be consistent with the time scales of electron–phonon coupling and energy transfer to the glass matrix. The corresponding rate equations were solved numerically using an arbitrary absorption cross section σ, because for saturation phenomena only the product σI of cross section and intensity I is important [23]. The results of the model calculations were finally compared to the data of Fig. 4 choosing an appropriate combination of relative intensities. The amplitude of the curves was scaled by an arbitrary, but common factor to meet the experimental values. The solid curves given in Fig. 4 refer to results obtained with $t_{\text{p}} = 200$ fs and the same relative intensities as those of the experimental data. Within experimental accuracy, measured and calculated curves agree nicely with each other. The saturation limit of extinction change obtained numerically using the same parameters, but significantly higher energy, is given as the dashed curve in Fig. 4. In general the described model calculations suggest that we interpret the observed bleaching, at least at these early delay times, to be caused by dynamic shift and/or broadening of the SP extinction band due to heating of the electron system. It should be noted that even for the highest energy density used in this work the absorption is not bleached completely during the excitation pulse; so an increase of the pump energy will in any case increase the amount of energy deposited in the sample and thus the electron temperature which can be reached as a consequence of the excitation. However, as in the very non-linear range of our experiments very high electron temperatures can be present, it is clear that the above simplified discussion serves as a model, but is not intended to be full description of the real physical processes.

4 Discussion

In this final section, some physical processes will be discussed which could correspond to the observed dynamics on the different time scales and, particularly, which of those could lead to deformation of the silver nanoparticles and formation of a halo of smaller silver clusters within the glass matrix. A further question arises considering the fact that the orientation of deformed particles was found to depend on the polarization of the laser pulses [11, 12]: whereas the reshaping process seems to happen on a time scale of several hundred ps, an orientational preference given by the linear polarization of the laser light is only present for the duration of the ultrashort pulse, i.e. typically 150 fs. Thus a very fast process must be supposed creating a more long-lived directional memory in the sample. So, in principle two kinds of scenario can be imagined to be consistent with the various observations: (i) the complete deformation happens within the time interval of interaction with the laser pulse, and any slower dynamics observed in our experiments is due to thermalization of the excess energy; (ii) the fs pulse does not directly deform the particles, but only creates a very high local energy density on the cluster and some kind of directional memory, and the structural modifications happen on the much slower time scale of some tens to hundreds of ps.

The plausibility of both ideas can be checked by discussing the time needed for material transport, which is in any case necessary for permanent modifications. In the first case, material (silver) would have to be transported over several nm within 150 fs. However, thermally induced ejection of Ag atoms or ions can be excluded for this interval of time, because heating of the silver lattice can only occur on the time scale of electron−phonon coupling, i.e will take several ps. A simple estimation shows that also direct emission of silver ions by the strong electric field of the laser pulse cannot manage the required ultrafast material transport: the applied maximum light intensity of $2 \times 10^{12}\,\text{W/cm}^2$ corresponds to an electric field amplitude of $\approx 4 \times 10^9\,\text{V/m}$; even if this would be a static electric field and the corresponding force could act on an isolated Ag^+ ion, it would take 750 fs to move this ion over a distance of 1 nm. In reality only the, in principle, possible $\chi^{(2)}$ process of optical rectification could provide such a static field, but this field is expected to be significantly weaker. So it can be concluded that the particle reshaping cannot be finished within the duration of the laser pulse. This is in accordance with the observed volume oscillations of the particles with a period of several ps [18–21].

Thus, clearly scenario (ii) must be favored, because in this case material transport is no problem due to the significantly longer time scales. However, still the possible processes being responsible for halo formation and particle deformation have to be discussed. As was shown recently on the example of small Na clusters theoretically [24] and experimentally [25], metal clusters can be ionized at laser intensities in the range of those applied in our study. Also, in the case of Ag clusters in liquid solution the ejection of electrons as consequence of a two-photon process was observed and discussed as the crucial process for photo-induced fragmentation of the clusters [6, 7]. The quadratic intensity dependence found there indicates a $\chi^{(2)}$ process; so optical rectification could play a role, and the dc electric field provided thereby could be responsible for electron ejection in a preferred direction. After thermalization of the electronic system, also a thermal (and thus more or less isotropic) ejection of electrons seems possible: for bulk silver, electrons need typically 4.5 eV to leave the surface, which corresponds to an electron temperature of 5×10^4 K. Such an electron temperature can well be reached under the given conditions, because even after equilibration with the Ag lattice formal temperatures of 10^4 to 10^5 K can be estimated for the whole silver particle [10]. Considering these high energy densities within the particle, which should affect the silver lattice after typically 10–20 ps, it may be assumed that also silver ions or small cluster fragments are then ejected into the glass matrix.

The further evolution clearly depends on (at least) two questions: (i) can the electrons leave the sample, are they

trapped in the matrix (and for how long) or do they return very quickly to the ionized clusters; (ii) is the energy density high enough to 'melt' the silver particle and the surrounding glass, and how long does it take to cool down particle and matrix below its 'freezing point' by thermal diffusion again? Starting with question (ii), it can be stated that, according to the above given numbers, obviously temperatures far above the melting temperatures of glass and silver are possible. Using typical values for density, heat capacity and heat conductivity of glass a thermal relaxation time of ≈ 200 ps is obtained for a temperature gradient having a characteristic length of 10 nm. So it seems plausible that the silver particle and its surroundings is in a 'molten' state for several hundred ps, or more precisely, the mobility of atoms and ions can be increased by several orders of magnitude in this interval of time. Concerning question (i), it is well known that even thermodynamically stable traps exist for electrons in glasses [26, 27]; so it seems very probable that at least a part of the ejected electrons is trapped in the glass matrix for a sufficiently long time, and they only recombine with the ionized clusters when these are frozen again.

The formation of a halo of small silver clusters is in reasonable agreement with this view of the nanoscopic situation. The deformation of the remaining particle, especially the elongation in a common direction with respect to the laser polarization, would in this picture be due to the Coulomb field of an anisotropic distribution of trapped electrons; the latter can only be produced by the discussed directed electron emission. On the other hand the volume oscillations observed in experiments without permanent modifications [18–21] should not be forgotten, since they should be excited in our experiments, too. If an anisotropic mode is excited, these oscillations could also be the beginning of particle deformation, particularly if one recalls the strong temperature increase within several ps: it can, for example, be imagined that at an arbitrary phase of the oscillation the elastic force is drastically reduced due to melting of the particle; if, in particular, the oscillation period is increased to a value significantly above the thermal relaxation time, the particle could be frozen in a rather definite shape. However, to clear this question more experimental and theoretical work will be required. Another important question to be worked upon in future is a possible chemical modification of the silver-glass interface, which could also contribute to the observed spectral shifts [9] or modify relaxation times [28]. From the present data no information on this problem can be deduced.

Finally, it is interesting to discuss which consequences this view of the nanoscopic situation would have for the interpretation of the observed time evolution of the extinction changes. Generally, a spectral shift due to the ionization of the Ag nanoparticles, and an excess absorption due to the trapped ('solvated') electrons has to be regarded. It is known that the removal of electrons from the Ag cluster leads to a redshift and slight broadening of the plasmon absorption [29]. On the other hand solvated electrons in a dielectric give rise to a broad absorption band in the visible, which may have a notable contribution at 400 nm [30]. Comparing these statements with the data of Fig. 3, the quite different dynamical behavior of transmission between 10 ps and several ns (stationary value) could be interpreted as a consequence of both dynamic spectral shift of the particles' SP band (due to ionization) and the band of ejected electrons, which of course must vanish again upon recombination with the silver ions. But a distinct assignment can not be given on the basis of the presented single-frequency data alone. More details about this topic can be expected from similar experiments using "white" (broad bandwidth) probe light, which are already in preparation in our laboratory.

Acknowledgements. This work was supported by the SFB 418 of the Deutsche Forschungsgemeinschaft.

References

1. T. Tokizaki, A. Nakamura, S. Kaneko, K. Uchida, S. Omi, H. Tanji, Y. Asahara: Appl. Phys. Lett. **65**, 941 (1994)
2. J.Y. Bigot, J.-C. Merle, O. Cregut, A. Daunois: Phys. Rev. Lett **75**, 4702 (1995)
3. T.S. Ahmadi, S.L. Logunov M.A. El-Sayed: J. Phys. Chem. **100**, 8053 (1996)
4. M. Perner, P. Bost, U. Lemmer, G. von Plessen, J. Feldmann, U. Becker, M. Mennig, M. Schmitt, H. Schmidt: Phys. Rev. Lett. **78**, 2192 (1997); G.V. Hartland, J.H. Hodak, I. Martini: Phys. Rev. Lett. **82**, 3188 (1998)
5. A. Brysch, G. Bour, R. Neuendorf, U. Kreibig: Appl. Phys. B **68**, 447 (1999)
6. M. Fierz, K. Siegmann, M. Scharte, M. Aeschlimann: Appl. Phys. B **68**, 415 (1999)
7. P.V. Kamat, M. Flumiani, G.V. Hartland: J. Phys. Chem. B **102**, 3123 (1998)
8. F. Gonella, G. Mattei, P. Mazzoldi, E. Cattaruzza, G.W. Arnold, G. Battaglin, P. Calvelli, R. Polloni, R. Bertoncello: Appl. Phys. Lett. **69**, 3101 (1996)
9. D.H. Osborne Jr., R.F. Haglund Jr., F. Gonella, F. Garrido: Appl. Phys. B **66**, 517 (1998)
10. M. Kaempfe, T. Rainer, K.-J. Berg, G. Seifert, H. Graener: Appl. Phys. Lett. **74**, 1200 (1999)
11. M. Kaempfe, H. Hofmeister, S. Hopfe, G. Seifert, H. Graener: submitted for publication
12. M. Kaempfe, T. Rainer, H. Hofmeister, K.-J. Berg, G. Seifert, H. Graener: to be published
13. see for example J. Zarzycki (Ed.): *Glasses and Amorphous Materials* (VCH, Weinheim 1991)
14. T. Klar, M. Perner, S. Grosse, G. von Plessen, W. Spirkl, J. Feldmann: Phys. Rev. Lett. **80**, 4249 (1998)
15. B. Lamprecht, A. Leitner, F.R. Aussenegg: Appl. Phys. B **68**, 419 (1999)
16. J.-Y. Bigot, V. Halté, J.-C. Merle, A. Daunois: Chem. Phys. **251**, 181 (2000)
17. J.H. Hodak, I. Martini, G.V. Hartland: J. Phys. Chem. B **102**, 6958 (1998)
18. M. Nisoli, S. de Silvestri, A. Cavalleri, A.M. Malvezzi, A. Stella, G. Lanzani, P. Cheyssac, A. Kofman: Phys. Rev. B **55**, 13424 (1997)
19. J.H. Hodak, I. Martini, G.V. Hartland: J. Chem. Phys. **108**, 9210 (1998)
20. S. Stagira, M. Nisoli, S. De Silvestri, A. Stella, P. Tognini, P. Cheyssac, R. Kofman: Chem. Phys. **251**, 259 (2000)
21. M. Perner, J. März, G. von Plessen, J. Feldmann, T. Porstendorfer, K.-J. Berg, G. Berg: In *Ultrafast Phenomena XI*, ed. by T. Elsaesser, J.G. Fujimoto, D.A. Wiersma, W. Zinth (Springer, Berlin, Heidelberg 1998)
22. N. Del Fatti, F. Vallé, C. Flytzanis, Y. Hamanaka, A. Nakamura: Chem. Phys. **251**, 215 (2000)
23. H. Graener, G. Seifert, A. Laubereau: Chem. Phys. Lett. **172**, 435 (1990)
24. F. Calvayrac, A. Domps, P.-G. Reinhard, E. Suraud, C.A. Ullrich: Eur. Phys. J. D **4**, 207 (1998)
25. R. Schlipper, R. Kusche, B. von Issendorff, H. Haberland: Phys. Rev. Lett. **80**, 1194 (1998)
26. B.P. Antonyuk, S.F. Musichenko: Phys. Scr. **58**, 83 (1998)
27. J.D. Prohaska, J. Li: Appl. Phys. Lett. **67**, 1841 (1995)
28. U. Kreibig, M. Gartz, A. Hilger, R. Neuendorf: Nanostruct. Mater. **11**, 1335 (2000)
29. A. Henglein, P. Mulvaney, T. Linnert, A. Holzwarth: J. Phys. Chem. **96**, 2411 (1992)
30. M. Kolodziejski, H. Abramczyk: J. Mol. Struct. **436**, 543 (1997)